



XXIII Congreso Español de Informática Gráfica

CEIG 2013

Editores

M^a Carmen Juan y Diego Borro

ISBN: 978-84-695-8333-3



CEIG 2013

Conference Chair

Miguel A. Otaduy Universidad Rey Juan Carlos

Program Chairs

Diego Borro Ceit y Tecnun (Universidad de Navarra)
M. Carmen Juan Universidad Politécnica de Valencia

Local Committee

Miguel A. Otaduy Universidad Rey Juan Carlos
Marcos Novalbos Universidad Rey Juan Carlos
Jorge Gascón Universidad Rey Juan Carlos

Program Committee

Francisco Abad	Universidad Politécnica de Valencia
Aiert Amundarain	Ceit - Centro de Estudios e Investigaciones Técnicas
Carlos Andujar	Universitat Politècnica de Catalunya
Dolors Ayala Vallespi	Universitat Politècnica de Catalunya
Imma Boada	Universitat de Girona
Diego Borro	Ceit y Tecnun (Universidad de Navarra)
Carles Bosch	Universitat de Girona
Pere Brunet	Universitat Politècnica de Catalunya
Eva Cerezo	Universidad de Zaragoza
Antonio Chica Calaf	Universitat Politècnica de Catalunya
Miguel Chover	Universitat Jaume I
Francisco R. Feito	Universidad de Jaén
Julián Flores	Universidad de Santiago de Compostela
Alex Garcia-Alonso	Universidad del País Vasco
Marcos García Lorenzo	Universidad Rey Juan Carlos
Diego Gutiérrez	Universidad de Zaragoza
Juan José Jiménez Delgado	Universidad de Jaén
M. Carmen Juan	Universidad Politécnica de Valencia
Domingo Martín	Universidad de Granada
Luis Matey Muñoz	Ceit y Tecnun (Universidad de Navarra)
Fco. Javier Melero Rus	Universidad de Granada
Ramón Mollá	Universidad Politécnica de Valencia

CEIG 2013

Adolfo Muñoz Orbañanos	Universidad de Zaragoza
Miguel A. Otaduy	Universidad Rey Juan Carlos
Gustavo Patow	Universitat de Girona
Francisco J. Perales	Universitat de les Illes Balears
Anna Puig Puig	Universitat de Barcelona
Immaculada Remolar	Universitat Jaume I
Mateu Sbert	Universitat de Girona
Rafael Jesús Segura	Universidad de Jaén
Francisco J. Serón	Universidad de Zaragoza
Antonio Susín	Universitat Politècnica de Catalunya
Juan Carlos Torres	Universidad de Granada
Pere-Pau Vazquez	Universitat Politècnica de Catalunya
Roberto Vivó	Universidad Politècnica de Valencia

Revisores adicionales

Iker Aguinaga	Ceit y Tecnun (Universidad de Navarra)
Antón Bardera	Universitat de Girona
José Iglesias	Universidad de Zaragoza
Juan Roberto Jiménez	Universidad de Jaén
Juan Antonio Magallón	Universidad de Zaragoza
Milan Magdics	Universitat de Girona
José María Noguera Rozúa	Universidad de Jaén

Preface

This volume contains the proceedings of the XXIII Spanish Computer Graphics Conference, held in Madrid, on September 17-20, 2013. The goal of this conference is to bring together the research results from the different Spanish groups on a wide range of topics, from animation to rendering, procedural modeling, medicine or augmented reality. In addition to providing a place to communicate new results, CEIG fosters interactions, and hopes to help define new productive directions for research and applications. We received 32 total submissions this year. Each submission was reviewed by at least three members of the International Program Committee or assigned external reviewers. Based on the reviews, we accepted 17 as full papers, 3 as educational papers, 2 as posters (modality 1) and 7 as posters (modality 2); scientific interest and innovation were the only selection criteria. All the accepted papers are to be presented orally at the conference, grouped in 6 sessions. Posters will be presented in one of these sessions. Each poster presentation will be preceded by a FastForward session where the authors briefly presented their works. The regular papers cover a wide range of topics. We have placed them in 5 sessions:

- Geometry and Levels of Detail
- Measurement and Visualization
- Vision and Imaging
- Animating Objects and Characters
- Games and Education

CEIG 2013 will also enjoy invited talks by renowned international researchers. This year, we are pleased to announce two highly successful young researchers in Europe: Prof. Christian Theobalt from Saarland University and the Max Planck Institute, and Prof. Niloy Mitra from University College London. Incidentally, both are recipients of a 2013 ERC Starting Grant. Prof. Theobalts research lies at the crossroads of computer graphics and computer vision, and in his talk he will discuss the capture, reconstruction, and modification of reality in motion. Prof. Mitra, recipient also of the 2013 ACM SIGGRAPH Significant New Researcher award, is pushing the boundaries of geometric analysis of shapes, 3D modeling techniques, and computational design tools.

New this year to CEIG, the program also includes activities to strengthen the collaboration between academia and industry in Spain. The program features two exciting roundtables. First, a selected group of entrepreneurs will share their experience in the creation of startup companies in the field of

CEIG 2013

computer graphics, ranging from videogame studios to technology providers. They will debate, among other topics, the role played by technological innovation in the creation of their startups. Second, representatives from the major computer graphics companies in Spain will debate about novel ways to collaborate with academia, including both research and educational aspects.

At the conference, the best papers will be selected and invited to submit an extended version to the Computer Graphics Forum journal, based on both the reviews and the presentations. All these papers will be reviewed again to ensure that they contain a sufficiently large amount of new material not covered in the CEIG version. We would like to thank everybody involved in organizing this conference, the authors of all submissions and the International Program Committee members and the external reviewers. This year, a primary reviewer was assigned to each paper. This primary reviewer was in charge of checking if the reviewers suggestions were considered for the final paper version. It has been an honor to serve as General Chair and Program Chairs of CEIG 2013, and we hope we have met the high standards that the conference demands.

CEIG 2103 General Chair

Miguel A. Otaduy (Universidad Rey Juan Carlos)

CEIG 2013 Program Chairs

M. Carmen Juan (Universidad Politécnica de Valencia, Spain)

Diego Borro (CEIT y Tecnun-Universidad de Navarra, Spain)

Table of Contents

Papers 1: Geometry and Levels of Detail

FractalHull: An incremental convex hull algorithm for 2D points	1
<i>Manuel García and Alejandro León</i>	
EBP-Octree: An optimized bounding volume hierarchy for massive polygonal models.	11
<i>Ángel Aguilera García, Francisco Feito Higuera and Francisco Javier Melero Rus</i>	
NavMeshes with exact clearance for different character sizes	21
<i>Ramón Oliva and Nuria Pelechano</i>	
City-Level Level-of-Detail	29
<i>Gonzalo Besuievsky and Gustavo A. Patow</i>	

Papers 2: Measurement and Visualization

Morpho-Volumetric measurement tools for abdominal distension diagnose	39
<i>Eva Monclús, Imanol Muñoz-Pandiella, Pere-Pau Vázquez, Isabel Navazo, Elisabeth Barba Orozco, Anna Accarino, Sergi Quiroga and Fernando Azpiroz</i>	
Extending neuron simulation visualizations with haptic feedback	49
<i>Laura Raya, Pablo Aguilar, Marcos García and Juan B. Hernando</i>	
Human-like Recognition of Straight Lines in Sketched Strokes	57
<i>Raquel Plumed, Pedro Company and Peter Varley</i>	
Measuring Surface Roughness on Cultural Heritage 3D models	67
<i>Luis López, Juan Carlos Torres and Germán Arroyo</i>	

Papers 3: Vision and Imaging

A Study of Octocopters for 3D Digitization from Photographs in Areas of Difficult Access	79
<i>Germán Arroyo, Alejandro Rodríguez and Juan Carlos Torres</i>	
Optimized generation of stereoscopic CGI films by 3D image warping. .	89
<i>Jose María Noguera, Antonio Rueda, Miguel A. Espada and Máximo Martín</i>	
A Client-Server Architecture for the Interactive Inspection of Segmented Volume Models	99
<i>Jordi Surinyac and Pere Brunet</i>	

CEIG 2013

Rendering Relativistic Effects in Transient Imaging.....	109
<i>Adrián Jarabo, Belen Masía, Andreas Velten, Christopher Barsi, Ramesh Raskar and Diego Gutiérrez</i>	

Papers 4: Animating Objects and Characters

Anisotropic Strain Limiting.....	121
<i>Fernando Hernández, Gabriel Cirio, Álvaro G. Pérez and Miguel A. Otaduy</i>	
Simulation of Hyperelastic Materials Using Energy Constraints.....	129
<i>Jesús Pérez, Álvaro G. Pérez and Miguel A. Otaduy</i>	
An interactive graphical tool for dressing virtual bodies based on mass-spring model, Verlet integration and raycasting.....	137
<i>José Ignacio Blanco Cruzado, José Pascual Molina Massó, Pascual Gonzalez, Jonatan Martínez Muñoz and Arturo Simón García Jiménez</i>	
Dynamic Footstep Planning for Multiple Characters.....	147
<i>Alejandro Beacco, Nuria Pelechano and Mubbasir Kapadia</i>	

Papers 5: Games and Education

An extensible framework for teaching Computer Graphics with Java and OpenGL.....	161
<i>Carlos Javier Ogayar, Juan José Jiménez Delgado and Jose María Noguera</i>	
Nuevo Grado en Diseño y Desarrollo de Videojuegos.....	167
<i>Inmaculada Remolar, Cristina Rebollo and Miguel Chover</i>	
Graphics Systems in a Software Engineering Curriculum.....	173
<i>Fco. Javier Melero</i>	
A Computer-Based Learning Game for Studying History.....	177
<i>Juan-Fernando Martín-Sanjosé, M. Carmen Juan, Juan Cano and M. Giménez</i>	

Posters

- Towards a 3D Cadastre 189
María Dolores Robles Ortega, Francisco Feito and Lidia Ortega
- Illumination of large urban scenes 191
María Dolores Robles Ortega, Juan Roberto Jiménez Pérez and Lidia Ortega
- *Cages: A MultiLevel, MultiCage Based System for Mesh Deformation
Francisco González García, Teresa Paradinas, Narcís Coll and Gustavo A. Patow
- Customizable LoD for Procedural Architecture
Gonzalo Besuievsky and Gustavo A. Patow
- Modeling and Estimation of Internal Friction in Cloth
Eder Miguel, Rasmus Tamstorf, Derek Bradley, Sara C. Schwartzman, Thomaszewski Bernhard, Bernd Bickel, Wojciech Matusik, Steve Marschner and Miguel A. Otaduy
- Rendering Light Transport in Transient-State
Julio Marco, Adrián Jarabo, Wojciech Jarosz and Diego Gutierrez
- Depicting Stylized Materials with Vector Shade Trees
Jorge López-Moreno
- What is the best interface to edit a light field? An Evaluation of Interaction Paradigms for Light Field Editing
Adrián Jarabo, Belen Masía, Adrien Bousseau, Fabio Pellacini and Diego Gutiérrez
- Large-Scale Multilevel Fluid Simulation with Localized FLIP
Iván Alduán Íñiguez and Miguel A. Otaduy

Human-like Recognition of Straight Lines in Sketched Strokes

R. Plumed¹, P. Company² and P. Varley²

¹Department of Mechanical Engineering and Construction, Universitat Jaume I, Castellón de la Plana, Spain

²Institute of New Imaging Technology, Universitat Jaume I, Castellón de la Plana, Spain

Abstract

In this study we consider approaches for recognising straight lines in sketches. We argue that the computer must attempt to match human perception rather than arbitrary geometric criteria. We describe an experimental procedure for comparing human and machine perception of straight lines, in order to determine which predictions from automatic recognition of straight lines are “good” (match human perception) and which are “bad”.

We evaluate and compare two well-known computational approaches: chord length and Hough transform, and conclude that both correlate moderately well with human perception of straight lines, but neither is good enough to consider this a solved problem. We propose instead a Normalised Hough Transform (NHT), which reliably produces acceptable results. We identify tuning parameters which allow this algorithm to replicate the human ability to accept and reject strokes.

We find that the NHT algorithm can produce reasonably good results with a single tuning parameter, but that by resolving borderline cases with two tuneable criteria we can improve performance still further: rejecting borderline cases with large oscillations and undulations helps to reject false positives, and the obliqueness of strokes also has a slight but measurable influence on its perception as a straight line.

Categories and Subject Descriptors (according to ACM CCS): J.6 [Computer-Aided Engineering]: Computer-Aided Design, I.5.2 [Design Methodology]: Classifier design and evaluation, I.4.6 [Segmentation]: Edge and feature detection.

1. Introduction

In this paper, we revisit the problem of straight line recognition. Traditionally, the first step in analysing a sketch is vectorisation: the input is a stroke, and the output is a line. Once lines have been identified (e.g. as straight lines or circumference arcs) the Sketch-Based Modelling (SBM) process may continue. We note that with some input devices converting sketched input into discrete strokes is itself non-trivial; this is discussed elsewhere, e.g. [HT06] and [BCF*08].

Various approaches have been proposed for stroke classification. Shpitalni and Lipson [SL97] apply linear least squares fitting to a conic section equation; the resulting ellipse or hyperbola is arbitrarily classified as a straight line if its aspect ratio exceeds 20:1. Qin [Qin05] proposes a method for classifying pen strokes based on adaptive thresholds and fuzzy knowledge with respect to curves' linearity and convexity. Zhang et al [ZSD*06] summarise older approaches, and propose a seeded segment growing algorithm for extracting graphical primitives from a stroke. They try to refine their control parameters by using relationships between primitives. Their algorithm is reportedly reliable for detecting straight segments.

However, the main conclusion here is that, to the best of our knowledge, the thresholds used in the literature were

estimated by the authors without taking into account how well they correlate with human perception.

In this paper, we seek to identify those parameters which help humans to recognise a stroke as a straight line.

We revisit two proposed solutions: the simplest, which compares chord lengths [QWJ01], and the most popular, using the Hough transform [DH72]. Since our ideal of a reliable algorithm is one which “perceives” exactly as humans do, we compare the two approaches with human interpretations of the same input data. Both approaches depend on tuning parameters, and we analyse the influence of tuning parameters on reliability. In contrast to previous attempts to tune these algorithms, we attempt to match human perception rather than a mathematical ideal.

We find that, although both correlate moderately well with human perception of straight lines, neither is good enough to consider this a solved problem.

We propose a new algorithm based on a modification to the Hough transform. Our results demonstrate that even with a single tuning parameter this fits better with human perception of straight lines. By applying more sophisticated criteria to resolve borderline cases, we can improve this performance still further.

Section 2 presents our test data: the human interpretation of strokes. Section 3 describes the three algorithms. Section 4 presents our results: how the algorithms interpret the

same input data, and how the algorithms can be tuned so that machine interpretations match human interpretations.

2. Human perception

As stated above, the main goal of this paper is to describe an algorithm which replicates the way humans recognise scribbled lines as depicting straight lines. One immediate difficulty is that human perception is influenced by different types of stimulus: by the drawing skill of the author, and by the observer's knowledge and capability in interpreting drawings.

Another problem we have noted is that different sketch recognition algorithms are typically tuned manually to fit their implementers' own drawing style and perception. Our challenge is to find a more general method, based on what most humans perceive.

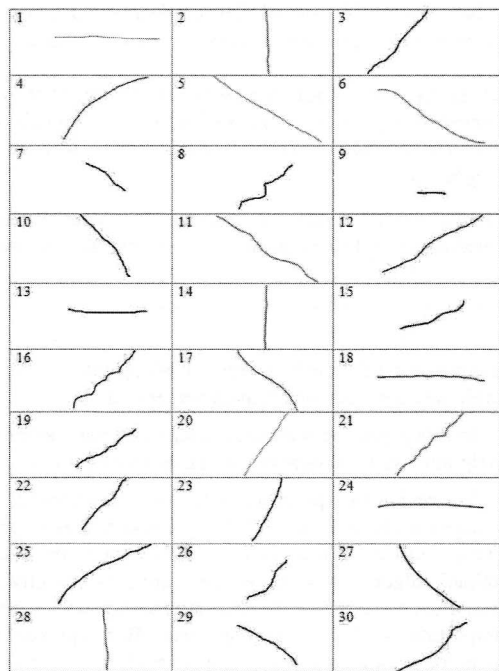


Figure 1: Example strokes (not to scale)

Our first step is to study and analyse human stroke recognition by performing experiments with groups of humans who are then interviewed to make their perceptions explicit.

Section 2.1 shows our input data. Sections 2.2, 2.3 and 2.4 describe the experiments performed using such questionnaires.

2.1 Initial data

This section describes the test data which we presented both to humans and to computer algorithms. We collated 30 example sketched strokes which include strokes of different nature and length (Figure 1). Each stroke is a list of sampled points, stored by their Cartesian x,y-coordinates.

Some of them depict horizontal and vertical lines (with differing degrees of accuracy), others are clearly slanted lines. Some of them have high values of curvature; others have little curvature.

Example	Points	Stroke length	Density (%)	Speed	Slope (degree)
1	53	782	7	1.39	-1.08
2	60	311	19	0.57	-88.51
3	67	214	31	0.31	47.34
4	136	413	33	0.29	36.22
5	393	904	43	0.25	-30.82
6	257	767	33	0.29	-31.09
7	93	120	78	0.07	-37.28
8	120	187	64	0.12	38.06
9	48	60	80	0.07	-0.69
10	73	183	40	0.23	-51.13
11	387	1801	21	0.54	-32.66
12	110	375	29	0.34	-149.54
13	101	167	60	0.11	-0.54
14	80	260	31	0.32	-91.71
15	57	163	35	0.18	22.31
16	210	286	73	0.09	40.35
17	75	394	19	0.28	-41.99
18	172	410	42	0.20	-1.92
19	121	175	69	0.11	31.55
20	194	619	31	0.34	54.33
21	257	540	48	0.21	41.66
22	76	170	45	0.20	48.38
23	23	171	13	0.76	-115.46
24	15	366	4	2.26	-0.86
25	23	244	9	0.74	31.75
26	98	137	72	0.10	48.27
27	18	203	9	1.00	-45.27
28	198	262	76	0.10	94.50
29	99	176	56	0.15	-32.93
30	38	197	19	0.32	38.06

Table 1: Characteristics of example strokes.

Table 1 shows some characteristics of the examples. The columns list:

- Example number (as shown in Figure 1).
- The number of points (i.e. x,y-coordinate pairs).
- The bounding length of the stroke (distance between endpoints).
- The density of points defining the stroke (calculated as the ratio of number of points to stroke length)—if the stroke has significant variations in its path, these variations can remain hidden by a lack of density.
- Drawing speed, calculated as the ratio of length of the stroke to the time taken to draw it. A higher speed produces a lower density (as shows the negative correlation in Table 3).
- Slope of the line (in degrees) which best fits the data points (using the linear regression method explained in Section 3.3).

2.2 First experiment

The purpose of our first experiment is to determine which strokes are perceived by human beings as straight lines. We can guess that length, obliqueness, and drawing irregularities such as undulations, oscillations and high curvature ratio might influence human perception.

The examples listed in Figure 1 were distributed in three questionnaires with ten pictures each (Figure 2). A total of 97 questionnaires were returned.

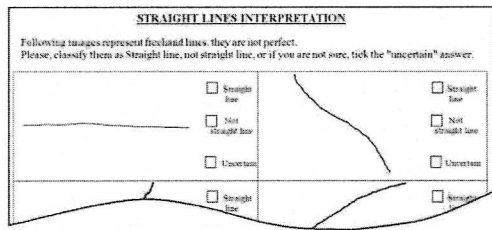


Figure 2: Questionnaire for the first experiment.

Most of the subjects were undergraduate students of industrial engineering or engineering design. Some subjects were academics from different technological areas. We also included a few subjects with no technical drawing training and a few subjects with no education beyond secondary level. Males and females were represented roughly equally.

The subjects were asked to classify the strokes of a questionnaire as depicting: straight lines (Yes), not straight lines (No) or uncertain (?). The results are tabulated in Table 2 as percentage of subjects who perceived them as straight lines. For each example we also list its length (already listed in Table 1, but reproduced here to ease comparisons), the linearity (obtained from the chord length algorithm explained in Section 3.1), the obliqueness and the tolerance.

Example	Yes (%)	No (%)	? (%)	Stroke length	Linearity (%)	Obliq.	Tol. (%)
1	97		3	782	99.66	0.024	1.93
2	97	3		311	98.39	0.033	1.96
5	97	3		904	93.06	0.685	2.62
24	94	6		366	99.65	0.019	3.30
14	91	9		260	97.23	0.038	1.59
20	91	9		619	94.89	0.793	2.56
28	91	9		262	94.97	0.100	3.63
13	78	19	3	167	96.79	0.012	3.70
9	76	21	3	597	93.93	0.015	5.36
18	75	25		410	96.92	0.043	3.79
22	47	44	9	170	91.83	0.925	5.77
23	41	47	1	171	97.58	0.566	6.59
3	39	52	9	214	94.58	0.948	6.44
21	28	72		540	87.60	0.926	6.57
12	25	59	1	375	94.92	0.677	5.07
19	25	69	6	175	86.61	0.701	5.96
29	22	69	9	176	89.15	0.732	8.28
10	18	73	9	183	93.58	0.864	8.88
27	16	75	9	203	97.76	0.994	9.64
25	9	81	9	244	96.79	0.706	10.13
7	9	82	9	120	83.80	0.829	11.00
17	6	84	9	394	95.79	0.933	8.49
15	6	91	3	163	91.07	0.496	10.14
11	3	94	3	180	94.58	0.726	6.46
30		94	6	197	94.49	0.846	10.81
4		97	3	413	92.24	0.805	13.16
6		97	3	767	93.49	0.691	7.42
8		97	3	187	79.45	0.846	14.09
16		100		286	82.06	0.897	8.55
26		100		137	85.23	0.927	16.52

Table 2: Results of the first experiment.

Obliqueness is a parameter which measures how slanted a stroke is (we cannot correlate slope directly because of its

non-linear behaviour). We define *obliqueness* as a normalised value in the range 0 (horizontal or vertical) to 1 (slope of 45 degrees). It is calculated from the slope data of the regression line fitted to the stroke and listed in Table 1 (it ranges between -180° and 180°) as follows:

if slope $\in \{-180^\circ \dots 0^\circ\}$, then slope $\leftarrow 180 + \text{slope}$;

if slope $\in \{90^\circ \dots 180^\circ\}$, then slope $\leftarrow 180 - \text{slope}$;

if slope $\in \{45^\circ \dots 90^\circ\}$ then slope $\leftarrow 90 - \text{slope}$;

$Obliqueness \leftarrow \text{slope}/45$

Tolerance is well known concept in Geometric Dimension and Tolerancing for measuring the “straightness” of a line. Given the bounding box of the line, defining x-range as the length of the side nearly parallel to the line and y-range as that of the side nearly perpendicular to the line, the absolute tolerance of straightness is the absolute value y-range, and the relative tolerance of straightness is the ratio y-range/x-range. The lower these parameters are, the straighter the stroke is considered to be. These parameters do not distinguish whether the lack of straightness results from oscillations or undulations (higher or lower frequency respectively).

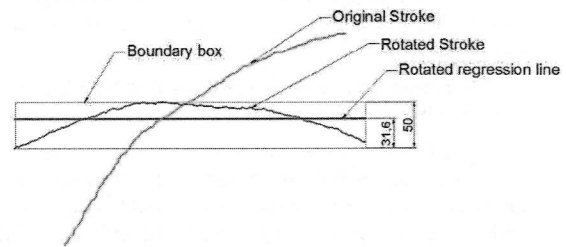


Figure 3: Regression line

The *tolerance* parameter measures the minimum bounding box which contains all the stroke points.

	Stroke length	Density (%)	Speed	Lin (%)	Obliq	Tol (rel)	Tol (abs)	Yes
Stroke length	Pear 1	-.320	.187	.198	.018	-.274	.824**	.053
	Sig.	.085	.323	.295	.926	.143	.000	.782
Density (%)	Pear	-.320	1	-.703	-.721*	.044	.221	-.237
	Sig.	.085	.000	.000	.818	.240	.208	.627
Speed	Pear	.187	-.703**	1	.556**	-.311	-.276	.018
	Sig.	.323	.000	.001	.095	.140	.923	.092
Linearity (%)	Pear	.198	-.721**	.556**	1	-.527**	-.609**	-.029
	Sig.	.295	.000	.001	.003	.000	.879	.002
Obliqueness	Pear	.018	.044	-.311	-.527**	1	.647**	.316
	Sig.	.926	.818	.095	.003	.000	.088	.000
Tolerance (rel)	Pear	-.274	.221	-.276	-.609**	.647**	1	.217
	Sig.	.143	.240	.140	.000	.000	.25	.000
Tolerance (abs)	Pear	.824**	-.237	.018	-.029	.316	.217	1
	Sig.	.000	.208	.923	.879	.088	.25	.013
Yes	Pear	.052	-.092	.314	.552**	-.760**	-.856**	-.446**
	Sig.	.785	.628	.092	.002	.000	.000	.013

Table 3: Pearson correlation

Figure 3 shows an original stroke and the computed regression line rotated to a horizontal orientation.

We applied Pearson correlation analysis to those parameters. Table 3 shows the results.

We find that relative tolerance correlates better with human perception (YES) than does absolute tolerance. For

this reason, from now on we use only relative tolerance and we abbreviate it to tolerance.

Although Table 2 shows that no stroke was always perceived as a straight line, examples 1, 2, 5, 24, 14, 20 and 28 were considered straight lines by more than 90% of subjects. Hence, we can conclude that low tolerance generally leads to high levels of perception of straightness.

Examples 13, 9 and 18 depict horizontal strokes with a medium tolerance due to a slight curvature and medium values of linearity, but even so, they were classified as straight lines by around 75% of the subjects. In contrast, example 12, which shows a relative medium tolerance but is oblique, was only perceived as straight line by around 25%.

The rest of the examples were considered as straight lines by less than 50% of the subjects. These strokes were drawn with different combinations of lengths and tolerances.

Examples 16 and 26 were invariably classified as not straight lines. These represent short strokes with noticeable high tolerances and low values of linearity. We can conclude that the combination of these factors is enough on its own to cause a stroke to be interpreted as not a straight line.

This preliminary analysis confirms that length does not influence human perception at all.

The analysis suggests that obliqueness does indeed affect the human perception of straight lines. Proving this requires a specific experiment, which should avoid any possible corruption in the sample due to the different abilities of drawer to draw lines with different slope. We discuss the result of this experiment in the next section.

2.3 Second experiment

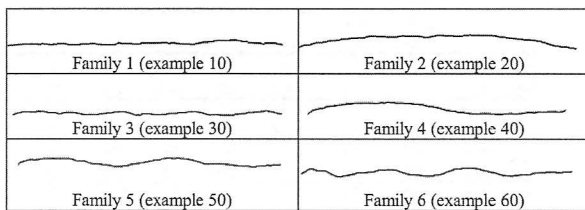


Figure 4: Strokes which define each family of lines

The goal in this section is to analyse and discuss the influence of the stroke’s obliqueness on the human perception of straightness. This general goal is specified in two hypotheses:

1. Slopes with no obliqueness (horizontal and vertical lines) are perceived in a similar way.
2. Vertical and horizontal directions are considered special directions which invoke in people the perception of straightness much more than do other values of obliqueness.

We created a test set of 72 examples which include 6 different families of stroke. Each family was generated by

rotating an original horizontal stroke. The horizontal strokes of each family are shown in Figure 4

Each family is characterised by parameters such as number of points, length, linearity and tolerance. The values of these parameters for each family are shown in Table 4.

Id family	Points	Length	%Linearity	Tol.
Family 1	641	760,79	94,51	1,71
Family 2	193	743,60	97,63	4,67
Family 3	578	686,10	91,54	2,20
Family 4	111	658,28	97,91	5,67
Family 5	301	799,64	95,93	3,80
Family 6	433	771,42	93,21	3,35

Table 4: General parameters of each family.

Each original stroke was rotated so that the regression line which best fits the stroke was oriented at the angles listed in Table 5 (thus each family contains twelve strokes). Each example is labelled by the Id angle defined in Table 5 followed by the number of its family.

Idangle	1	2	3	4	5	6	7	8	9	10	11	12
Angles	0°	9°	27°	45°	54°	72°	90°	99°	117°	135°	144°	162°
Obliq.	0	0.2	0.6	1	0.8	0.4	0	0.2	0.6	1	0.8	0.4

Table 5: Values of the angles used in the experiment

With regard to the questionnaires:

1. Each questionnaire contained twelve different examples chosen randomly, without any repetition. Each example appears in two different questionnaires. At the end, we created twelve different questionnaires.

2. The answer form contained the instructions for the experiment. It also contained a Likert-type scale to score the “straightness” of each figure. Each subject scored each example with a value from 5 (the figure was perceived as a straight line) down to 1 (the figure was perceived as not a straight line).

Figure 5 shows an example of questionnaire and an answer form.

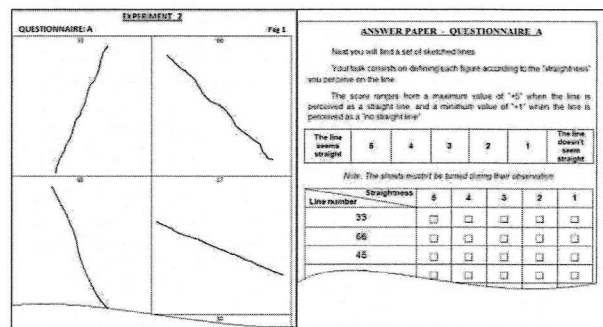


Figure 5: Example of questionnaire and answer form for the second experiment.

We collected a total of 144 answer forms, and obtained 24 perception data for each type of questionnaire and 48 perception data for each stroke (i.e combination of family and obliqueness).

Statistically, as we have the same number of data in each classification, the power of the method is maximised. In addition, our questionnaire design ensures that observa-

tions are independent. However, the number of samples was not enough for the requirements of each population's normal distribution and equality of variance to be satisfied.

To verify the first hypothesis, we used an ANOVA [HAT*98] taking as main factors the family identification and the slopes, using only the angles 0° and 90°, to obtain a 2x6 classification table. The ANOVA results are shown in Table 6.

Test of inter-subjects
Dependent variable: Straightness score

Origin	Sum of Square type III	df	Mean	F	Sig.
Corrected model	205.927a	11	18.721	20.141	0.000
Intersection	2194.531	1	2194.531	2360.983	0.000
Idfamily	195.323	5	39.065	42.028	0.000
Slope	3.337	1	3.337	3.590	0.059
Idfamily * Slope	7.267	5	1.453	1.564	0.170
Error	256.542	276	0.929		
Total	2657.000	288			
Corrected total	462.469	287			

a. R squared = 0.445 (R squared and corrected = 0.423)

Table 6: ANOVA results for first hypothesis

We deduce that whereas the groups defined by the factor Id_{family} have perception score means considerably different (Sig = 0.000 < 0.05), the factor Slope does not have a significant effect over the perception score mean (Sig = 0.059 > 0.05) and neither does the interaction Id_{family}*Slope (Sig = 0.17 > 0.05).

Therefore, the first hypothesis has been confirmed: horizontal and vertical slopes are perceived similarly.

To test the second hypothesis we applied an ANOVA, taking as main factors the family identification and all six levels of obliqueness, to obtain a 6x6 classification table. The results are shown in Table 7.

Test of inter-subjects
Dependent variable: Straightness Score

Origin	Sum of Square type III	df	Mean	F	Sig.
Corrected model	1141.298 ^a	35	32.609	35.320	0.000
Intersection	13139.598	1	13139.598	14232.213	0.000
Idfamily	1055.621	5	211.124	228.680	0.000
Obliq.	47.385	5	9.477	10.265	0.000
Idfamily *Obliq	38.292	25	1.532	1.659	0.022
Error	1562.104	1692	0.923		
Total	15843.000	1728			
Corrected total	2703.402	1727			

a. R squared = 0.422 (R squared and corrected = 0.410)

Table 7: ANOVA results for second hypothesis

The results suggest that both factors have a significant effect over the perception of straightness (in both cases Sig = 0.000 < 0.05). Therefore, the different families of lines are perceived as having different straightness, and the different members of the same family are also perceived differently—both the quality and the direction of the line influence the perception of straightness.

In addition, the interaction factor Id_{family}*Obliqueness shows a significant level of Sig = 0.022 (lower than 0.05), which means that even within the same family, the perception of straightness differs according to the obliqueness.

However, the weight of the Obliqueness variable is nowhere near as strong as that of the Id_{family} variable, as the high F-test value shows in the case of Id_{family} (F = 228.68) as opposed to the low value for Obliqueness (F = 10.265).

We can accept then that although obliqueness seems to affect the way people tend to perceive the straightness of a line, it should be considered as a secondary factor, not as important as those parameters which characterise the different families. The model with only these two main factors would only explain 42.2% (value of R squared) of the variations in the answers.

Straightness Score

Tukey B^{a,b}

Obliqueness	N	Subset		
		1	2	3
0,2	288	2.54		
0,4	288	2.56		
0,0	288		2.76	
0,6	288		2.80	
0,8	288		2.88	2.88
1,0	288			3.01

The table shows the means of the groups of homogeneous subsets.

a. It uses the simple size of the harmonic mean = 288.000

b. Alpha = 0.05

Table 8: Post hoc analysis, homogeneous groups.

Table 8 shows the results of a Tukey post-hoc analysis [DV99] which groups the different levels of obliqueness according to the similarity of their scoring means. As we can see, strokes with low but non-zero value of obliqueness have the lowest mean; their scores are nearly 5% lower than the mean scores of the second subset (which includes strokes with zero obliqueness); in contrast, the third subset, which groups the highest levels of obliqueness, has mean scores around 3% higher than the second subset.

Thus, regarding our second hypothesis, we can conclude that obliqueness does indeed seem to influence the perception of straightness, but, contrary to our expectations, people seem to be more sensitive to lack of straightness for lines close to horizontal or vertical. They are less demanding when the line depicts a slope around 45° or 135°.

3. Algorithms

In this section, we describe three algorithms for detecting straight lines from strokes. Our goal is to demonstrate the feasibility of defining perceptually-rooted parameters and their significance thresholds for such algorithms, taking into account the analysis made for human behaviour described in Section 2. In addition we shall compare the reliability of the algorithms.

In each case, our input data is a temporally-ordered list of sampled points captured in a single sequence: pen-down, pen-move, and pen-up.

3.1 Chord length

We study the chord length algorithm, based on the linearity parameter used by Qin et al. [QWJ01] to identify straight lines from an input data polygon. We have chosen this algorithm because of its ease of implementation and its very low computational cost

Linearity of a stroke is the ratio of the distance between the two end points to the sum of the distances between consecutive points.

The value of linearity lies between 0 and 1. A strict straight line has a linearity of 1. True straight lines rarely occur in freehand sketches, so we need to determine a tolerance in order to classify an input stroke. Our algorithm will identify a stroke as a straight line if its linearity is greater than a threshold. The explanation of how this threshold is set is in Section 4.

3.2 Hough Transform

The Standard Hough Transform (SHT) is an algorithm widely used to solve line detection problems in image processing and computer vision.

This was introduced by Hough in 1962, but all versions of the algorithm in use today are based on the Standard Hough Transform (SHT) of Duda and Hart [DH72]. Here, we study an adaptation of the SHT for rapid processing of a single pen input stroke [Lee06].

The algorithm represents a line as a linear equation in normal form, where the normal for a given line is the shortest segment between the line and the origin:

$$\rho = x \cos \theta + y \sin \theta \quad (1)$$

In this expression, θ represents the angle of inclination of the normal and ρ is the length of the normal. With these parameters fixed, x and y represent the Cartesian coordinates of each point which belongs to this straight line.

Using the normal form, we can represent each point in (x,y) space as a sinusoidal curve in (θ,ρ) space. Applying this procedure to every point, we obtain a set of sinusoidal curves.

All the sinusoidal curves which intersect at a particular point in (ρ, θ) space represent points which belong to the same straight line. The algorithm proposed by Lee [Lee06] discretises (ρ, θ) space into a finite number of cells, using an accumulator ρ - θ array where each cell is a counter which is incremented whenever a sinusoidal curve passes through it.

In the matrix, θ takes values between 0° and 180° with one cell per degree. The range of ρ is determined by doubling the length of the diagonal which frames the input stroke, and adding one to get an odd value:

$$\rho = 2 \sqrt{x_{\text{range}}^2 + y_{\text{range}}^2} + 1 \quad (2)$$

The known advantage of the SHT algorithm is its robustness. However, the algorithm also has weaknesses. First, as we work with freehand strokes, we need some flexibility to tolerate inaccuracies. Furthermore, the accuracy

of the results depends on the stroke length: the longer the stroke, the higher the value of ρ , and the better the accuracy. Secondly, stroke inclination affects ρ , as the variations of the parameters x_{range} and y_{range} (equation 2) change with varying inclination, so the same stroke is evaluated differently if its inclination changes. Finally, the algorithm requires more computation than the chord length algorithm, and increasing the precision requires more columns in the ρ - θ matrix, further increasing the computational cost.

In order to avoid these problems, we propose a modification to the Standard Hough Transform, the Normalised Hough Transform (NHT), where the difference is how the matrix parameters are defined. In the NHT, the discretisations of ρ and θ are fixed before running the algorithm, so the algorithm does not depend on the number of points in the stroke. In addition, the stroke is pre-rotated until we get its most likely horizontal direction (this process is described in Section 3.3). This allows us to determine a fixed tolerance value, independent of the length, the slope and number of points in the stroke.

The size of the ρ - θ matrix remains to be determined (this will be done in Section 4).

3.3 Stroke Pre-Rotation for NHT algorithm

In order to get the rotated stroke, the original stroke must be rotated so that it is (more or less) horizontal. But strokes are not straight lines, so determining the rotation angle is non-trivial: we must fit a straight line to the stroke data, and use its orientation as the rotation angle.

For this, we used *orthogonal regression* (OR), which minimises the sum of the squared orthogonal distances from the stroke data points to the fitting line. This is a natural generalisation of the least-squares approximation when the data in both variables, x and y , is perturbed. Other methodology closely related with OR is the Principle Component Analysis (PCA). Both methods obtain the same fitting line. We used OR method because our input data ease its application.

In order to convert our orthogonal regression into a simple linear regression problem, we adapt Brown's idea of seeking the principle directions of the data points [Bro12], but in our case we rotate the entire set of n points about the centroid. The rotation angle θ , which rotates the regression line so that its perpendicular corresponds to the vertical, is then calculated by minimising the sum of squares of the vertical heights of the n transformed data points.

4. Comparison between human perception and algorithmic classification

In this section we analyse the influence of rotation and obliqueness on the ability of algorithms to mimic human perception.

4.1 Influence of stroke rotation

To measure the influence of stroke rotation in the performance of the algorithms, we chose two strokes (16 and 18) and rotated them to get three different variants (Figure 6). We evaluated the six resulting strokes with four algorithms (Chord Length, SHT, Unrotated NHT, Rotated NHT). Table 9 collates the results of how those strokes were evaluated by the different algorithms.

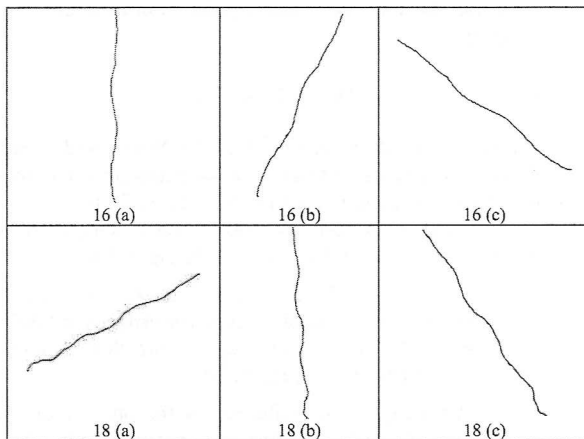


Figure 6: Strokes presented in different orientations.

As Table 9 shows, the Chord Length and the Rotated NHT algorithms can be considered robust, because (unlike the SHT and Unrotated NHT) they give a consistent value independent of the stroke orientation. Hence, we can discard Unrotated NHT, and all subsequent references to NHT are to Rotated NHT. SHT is also sensitive to rotation, but we shall not yet discard it, as we still wish to identify its other strengths and weaknesses.

Example	Slope	Linearity	SHT STIR%		
			No rotated	Rotated	
16.a	89°	95.93	10.30	50.83	50.83
16.b	64°	95.93	12.29	55.48	50.83
16.c	142°	95.93	14.62	53.82	50.83
18.a	28°	93.21	9.24	47.11	50.12
18.b	94°	93.21	9.70	45.73	50.12
18.c	123°	93.21	9.70	52.19	50.12

Table 9: Results of algorithms applied to Figure 6.

4.2 Tuning the algorithms

In order to find accuracy thresholds for the algorithms described in Section 3, we compare the output of each algorithm with the results of human perception of experiment 1. Table 10 shows our results. It is subdivided into three groups:

- examples considered as straight lines by human perception in more than 90% of cases.
- examples considered as straight lines in 50% to 90% of cases.
- examples considered as straight lines in less than 50% of cases.

Table 11 shows the Pearson correlations coefficients between the output of the algorithms and the initial input parameters. Table 12 shows the correlation coefficients between the results obtained with each algorithm and the human perception results.

Example	Yes %	Chord length	SHT	NHT	Obliq	Tol*COB
		Linearity %	STIR %	STIR %		
1	97	99.66	28.30	88.68	0.024	1.89
2	97	98.39	30.00	58.33	0.033	1.92
5	97	93.06	10.69	61.83	0.685	2.46
24	94	99.65	46.67	60.00	0.019	3.23
14	91	97.23	33.75	67.50	0.038	1.56
20	91	94.89	12.89	71.13	0.793	2.35
28	91	94.97	28.79	66.16	0.100	3.60
13	78	96.79	54.46	67.33	0.012	3.62
9	76	93.93	52.08	52.08	0.015	5.24
18	75	96.92	19.19	53.49	0.043	3.72
22	47	91.83	27.63	38.16	0.925	5.21
23	41	97.58	26.09	47.83	0.566	6.34
3	39	94.58	22.39	38.81	0.948	5.80
21	28	87.6	11.67	49.42	0.926	5.93
12	25	94.92	17.27	43.63	0.677	4.76
19	25	86.61	22.31	39.67	0.701	5.57
29	22	89.15	24.24	46.46	0.732	7.69
10	18	93.58	27.40	46.58	0.864	8.06
27	16	97.76	33.33	50.00	0.994	8.68
25	9	96.79	26.09	47.83	0.706	9.45
7	9	83.8	24.73	35.48	0.828	10.04
17	6	95.79	18.67	26.32	0.933	9.15
15	6	91.07	19.30	40.00	0.496	8.28
11	3	94.58	6.20	51.68	0.726	6.00
30	0	94.49	23.68	37.50	0.846	11.98
4	0	79.45	18.33	43.19	0.805	6.80
6	0	92.24	17.65	29.17	0.691	13.19
8	0	93.49	12.84	32.86	0.846	7.78
16	0	85.23	22.45	39.80	0.897	14.94
26	0	82.06	14.76	36.84	0.927	9.75

Table 10: Algorithm results against human perception

4.2.1 Chord Length

Linearity shows results obtained using the chord length algorithm. Qin et al [QWJ01] used a threshold of 95%, a value in accordance with the middle group of examples. With this value, we get one false negative (example 5) and six false positives (examples 13, 18, 23, 27, 25 and 17).

We note a high negative correlation (-0.721) between the Linearity and the Density (see Table 11), which suggests that Density is an influence in false results. Examples 17, 23, 25 and 27 have very low densities, and all depict lines with high curvature. It appears that piecewise linear approximation of a scribbled line input is unreliable in these cases—the chord length algorithm will classify smooth curved strokes as straight lines even when the curvature is high enough for humans not to perceive them as straight lines.

Stroke length has no effect on the results of the chord length algorithm. So, in this aspect, the algorithm behaves as humans do.

		Stroke length	Density	Obliq.	Tol.	SHT column	SHT linearit	NHT STIR	NHT STIR
Stroke length	Pear	1	-.320	.018	-.274	.999**	.198	-.514**	.256
	Sig.		.085	.926	.143	.000	.295	.004	.172
Density	Pear	-.320	1	.043	.221	-.347	-.721**	.062	-.212
	Sig.	.085		.820	.240	.060	.000	.744	.261
Obliq.	Pear	.018	.043	1	.647**	-.010	-.527**	-.607**	-.674**
	Sig.	.926	.820		.000	.959	.003	.000	.000
Tol.	Pear	-.274	.221	.647**	1	-.295	-.609**	-.240	-.714**
	Sig.	.143	.240	.000		.114	.000	.202	.000
SHT column	Pear	.999**	-.347	-.010	-.295	1	.236	-.490**	.280
	Sig.	.000	.060	.959	.114		.209	.006	.133
Linearity	Pear	.198	-.721**	-.527**	-.609**	.236	1	.370*	.547**
	Sig.	.295	.000	.003	.000	.209		.044	.002
SHT STIR	Pear	-.514**	.062	-.607**	-.240	-.490**	.370*	1	.335
	Sig.	.004	.744	.000	.202	.006	.044		.070
NHT STIR	Pear	.256	-.212	-.674**	-.714**	.280	.547**	.335	1
	Sig.	.172	.261	.000	.000	.133	.002	.070	

*. Correlation is significant at 0.05 level (bilateral).

** Correlation is significant at 0.01 level (bilateral).

Sample size is N=30

Table 11: Pearson correlation between output and input parameters.

Table 12 shows specifically the correlations between the different approaches and the results of human perception (YES). In the case of linearity the correlation is positive but insufficiently strong.

		Linearity	SHT	NHT	Yes
Linearity	Pearson	1	.370*	.547**	.552**
	Sig.		.044	.002	.002
SHT	Pearson	.370*	1	.335	.444*
	Sig.	.044		.070	.014
NHT	Pearson	.547**	.335	1	.827**
	Sig.	.002	.070		.000
Yes	Pearson	.552**	.444*	.827**	1
	Sig.	.002	.014	.000	

*. Correlation is significant at 0.05 level (bilateral).

Table 12: Pearson correlation between output and perception of experiment 1.

We conclude that although linearity parameter is easy to calculate using the chord length algorithm, it produces occasional false positives and negatives and, even worse, systematic false positives for smooth curves of low density.

4.2.2 Standard Hough Transform

The results of the Standard Hough Transform algorithm are shown in the SHT column of Table 10. The parameter shown is the signal-to-input ratio (STIR), i.e. the number of sinusoidal curves which intersect at a particular cell of the ρ - θ matrix.

It is not obvious how to find an appropriate threshold from these results.

It appears that the false results depend on the stroke length (and the derived parameter SHT columns in Table 1). Examples 5 and 20 have very high values of SHT columns, so the SHT algorithm is stricter than humans when classifying long strokes as lines. The false positive examples have low values of SHT columns, making the SHT

algorithm less strict than humans when classifying short strokes as lines.

Table 11 shows that there is no correlation between the result of Signal-to-Input ratio of SHT and the tolerance.

Table 12 shows that, overall, SHT has a weak correlation with human straight line perception, and if we also take into account the fact that the algorithm evaluation depends on the stroke direction, we can conclude that this algorithm does not allow us to obtain a good estimation of stroke straightness.

4.2.3 Normalised Hough Transform

First, as noted in Section 3.2, the Normalised Hough Transform requires additional tuning parameters: the number of rows and columns of the ρ - θ matrix. To this end, we analysed the signal-to-input ratio for each example in experiment 1 with several versions of the algorithm:

- We analysed the influence of the number of rows (i.e. discretisation of θ which corresponds to fidelity in rotation/inclination), by varying this parameter from 91 to 361 in steps of 30.
- We analysed the influence of the number of columns (i.e. discretisation of ρ which corresponds to fidelity in stroke length), by varying this parameter from 31 to 1199 in steps of 4.

We obtained the STIR for each stroke example and each combination of parameters, and compared them with the percentage of human perception as a straight line (see Table 10).

We find that human beings are more decisive than algorithms when evaluating good quality or bad quality strokes. The NHT algorithm frequently finds some residual straightness when humans completely reject a bad stroke, and when the size of the accumulator matrix cells are small enough, the algorithm will find some imperfections even when most of human beings ignore them and perceive the stroke as a good straight line.

As a consequence, we assume that discrepancy between humans and the algorithm is higher for very good and very bad quality strokes than it is for average quality ones. This means that the tuning parameters which fit the NHT algorithm to human perception are different for the three ranges. Since the threshold which distinguishes between strokes representing straight and not straight lines clearly belongs in the intermediate range, we removed the good and bad strokes and concentrated our further analysis on average strokes.

The best matches between NHT STIR and human perception occur when threshold values are between 5% and 95%.

Considering only those examples within this range, we summarised the results of each combination (each particular pair of number of rows and number of columns) as a single parameter: the absolute differences between the results as calculated by NHT algorithm and as perceived by humans (%YES). Figures 7 and 8 respectively show how

this parameter varies with respect to different numbers of rows and columns. The lower the difference, the better STIR correlates to human perception. Therefore, the minimum function value gives us the best choices for rows and columns.

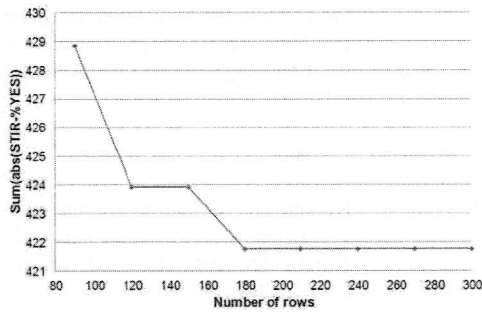


Figure 7: Influence of number of rows.

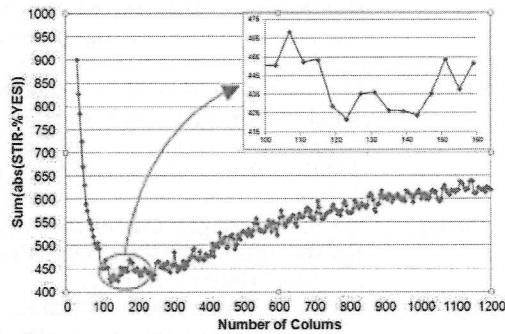


Figure 8: Influence of number of columns.

Analysing Figures 7 and 8, we chose a 180x143 matrix size, which minimizes the difference between STIR and %YES (the minimum values is 423.94). In subsequent experiments with NHT, we used 180x143 ρ - θ matrix

The results of the STIR of the Normalised Hough Transform algorithm are shown in the NHT column in Table 10. As Table 12 shows, this algorithm has a high (0.827) and significant (at 0.01 level) correlation with human perception. Using a threshold of 52%, there are no false negatives, and no false positives.

However, there are two borderline examples (9 and 18) which are close to being false negatives, with NHT STIR of 52.08 and 53.49 respectively.

There are also two examples (11 and 27) for which the STIR value is very close to the threshold value. These are characterised by having a high value of tolerance (6.46 and 9.64 respectively). According to Table 3, tolerance and positive results of human perception (YES) maintain a high negative correlation (-0.858) at 0.01 level. If we modify the algorithm by adding the extra condition that the tolerance must be lower than a certain threshold value for us to consider a borderline stroke as a straight line, all of the doubtful cases can easily be resolved.

Finally, it seems that obliqueness influences perception of strokes as straight lines, so perhaps obliqueness should

also be considered when determining the threshold value for tolerance.

4.2.4 Replicating obliqueness distortion in straightness perception

As a conclusion of our second experiment (Section 2.3), we stated that the orientation of the line influences the human perception of straightness. We want our algorithm to replicate this. Hence, we define a variable tolerance threshold which becomes stricter for orientations easily perceived by humans, and relaxes for orientations poorly perceived by humans.

In the light of the ANOVA analysis results (Table 7) the Obliqueness factor could be considered a secondary factor as its weight (F-test value) is roughly 20 times lower than the weight of the factor which defines the type of stroke (NHT STIR). For this reason, we defined a Coefficient of Obliqueness (COB) which affects the threshold value depending on the stroke's obliqueness.

According to Table 8, people seem to be strictest when obliqueness is around 0.2 (strokes close to the horizontal or vertical directions), and least strict when obliqueness reaches 1 (slope of 45°). From Table 8, the perceptual variation between the maximum value (3.01 for obliqueness of 0.8) and the minimum one (2.54 when obliqueness is 0.2) is 9.4%, so we suggest use of one coefficient which will affect the threshold value by up to 10% of its value.

In order to model our Coefficient of Obliqueness so that it behaves similarly to humans, we use a sinusoidal function where the input variable (x) is the stroke's obliqueness (Figure 9). The maximum value (at obliqueness 0.2) is 1.0, and the minimum value (at obliqueness 1.0) is 0.9. This function has been chosen for its characteristic of continuity between two extreme values, and its ease to be adapted to the behaviour we seek.

$$COB = \sin((x+0.125)(4\pi/3))/20 + 0.95 \quad (3)$$

Where the frequency of the wave is defined as 2/3, the peak deviation of the function from the average value will be 5%, which means that the amplitude must be 1/20, and the average value to which the wave oscillates is 0.95. In order to get the maximum value of deviation when obliqueness is 0.2, we introduced a phase lag in the wave of 0.125.

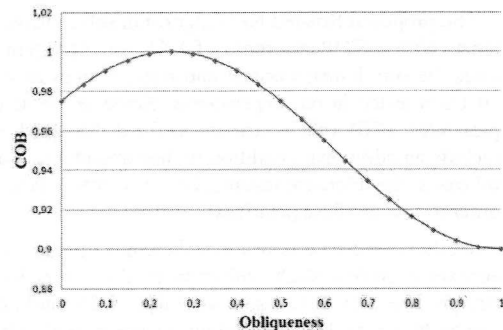


Figure 9: Coefficient of Obliqueness.

We apply the COB only to the NHT tolerance parameter. We do not apply it to the NHT primary threshold since NHT is a robust algorithm and the influence of the stroke's direction has been removed by pre-rotation to the horizontal. We do not apply it to the Chord Length algorithm because this only depends on chord and edge lengths which do not depend on the orientation of the stroke. And we do not apply it to the SHT because this already depends on the orientation of the stroke.

The results of tolerance for the first experiment taking into account the varying threshold are shown in the column "Tol*COB" of Table 10.

As can be seen in Table 10, all examples perceived as straight lines by more than 75% have a tol*COB maximum value of 5.3. Therefore our preferred algorithm includes a secondary condition such that a stroke must have a NHT STIR higher than 52% and also a tol*COB parameter lower than 5.3 to be classified as a straight line.

5. Conclusions

In this study we propose that recognition of straight lines should match human perception, rather than the intentions of the designer who produced the sketch.

We compare two algorithms for detecting straight lines: the simplest (chord length) and the most popular (Hough transform). We conclude that neither can be easily tuned so that machine interpretations replicate human interpretations. Instead, we propose a new algorithm based on a modification of the Hough Transform which matches human interpretations acceptably well.

Chord length (when tuned with a linearity threshold of 95%) has a reasonable correlation with human perception, but some false positives and negatives still appear. More worryingly, systematic false positives occur for smooth curves of high curvature (lines with undulations and without oscillations). We conclude that this approach should be avoided, as it ignores important perceptual assumptions.

SHT correlates poorly with human perception, and even finding an appropriate threshold for signal-to-input ratio (STIR) value is problematic. Small variations in STIR threshold produce very different classification results. Instead, we should use an approach which is less sensitive to the analysed parameters.

The proposed Rotated NHT algorithm solves these problems. With a STIR threshold of 52%, the algorithm replicates the way humans accept and reject strokes as lines in all cases tested in our experiments. However, some examples have STIR values near the defined threshold, so we include an additional condition to discriminate such doubtful cases: the tolerance threshold must be lower than 5.3 in order to prevent false positives.

We have also determined that the obliqueness of strokes appears to have a slight influence on the perception of a straight line. For this reason, we vary the threshold of tolerance by up to 10% depending on the stroke's oblique-

ness, using the Coefficient of Obliqueness described in section 4.2.4.

Acknowledgements

This work was partially funded by financial support from the Ramon y Cajal Scholarship Programme and by the "Pla de Promoció de la Investigació de la Universitat Jaume I", project P1 1B2010-01.

References

- [HT06] HILAIRE X., TOMBRE K.: Robust and accurate vectorization of line drawings, *IEEE Trans. Pattern Analysis and Machine Intelligence*, 28 (6), (2006) 890-904.
- [BCF*08] BARTOLO A., CAMILLERI K. P., FABRI S. G., BORG J. C.: Line tracking algorithm for scribbled drawings., 3rd Int. Symposium on Communications, Control and Signal Processing, (2008), pp 554-559.
- [SL97] SHPITALNI S., LIPSON H.: Classification of sketch strokes and corner detection using conic sections and adaptive clustering. *Trans. ASME J. Mech. Design*, 119 (2), (1997) 131-135.
- [Qin05] QIN S. F.: Intelligent Classification of Sketch Strokes. *IEEE EUROCON2005 "Computer as a Tool"*, (2005) 1374-1377.
- [ZSD*06] ZHANG X., SONG J., DAI G., LYU M.R.: Extraction of line segments and circular arcs from freehand strokes based on segmental homogeneity features. *IEEE Trans. Systems, Man, and Cybernetics*, 36 (2), (April 2006)
- [QWJ01] QIN S. F., WRIGHT D. K., JORDANOV I. N.: On-Line Segmentation of Freehand Sketches by Knowledge-Based Nonlinear Thresholding Operations. *Journal. Pattern Recognition*, 34 (10), (2001) 1885-1893.
- [DH72] DUDA R. O., HART P.E.: Use of the Hough Transformation to Detect Lines and Curves in Pictures. *Communication of the ACM*, 15, (1), (1972) 11-15.
- [HAT*98] HAIR J. F., ANDERSON R. E., TATHAM R. L., BLACK W.: *Multivariate Data Analysis*, Fifth edition. Prentice Hall International Inc., 1998.
- [DV99] DEAN A., VOSS D.: *Design and Analysis of Experiments*, Springer-Verlag New York, 1999, pp. 78-85
- [Lee06] LEE K.: Application of the Hough Transform, Unpublished Research Paper No. 2006-005, University of Massachusetts Lowell, Dept. of Computer Science, Lowell, MA 01854, (2006).
- [Bro12] BROWN K.: Perpendicular Regression of a Line. in *MathPages*. www.mathpages.com/home/kmath110.htm Accessed, February 2012.